Structural and Mechanistic Investigation of 3-Deoxy-D-*manno*-octulosonate-8-phosphate Synthase by Solid-State REDOR NMR†

Lilia Kaustov,‡ Shifi Kababya,‡ Schoucheng Du,‡ Timor Baasov,*,‡ Sara Gropper,§ Yuval Shoham,§ and Asher Schmidt*,‡

Department of Chemistry, Institute of Catalysis Science and Technology, and Department of Food Engineering and Biotechnology, Technion-Israel Institute of Technology, Haifa 32000, Israel

Received July 24, 2000; Revised Manuscript Received September 20, 2000

ABSTRACT: $^{15}N\{^{31}P\}$ REDOR NMR experiments were applied to lyophilized binary complexes of 3-deoxy-D-*manno*-2-octulosonate-8-phosphate synthase (KDO8PS), with each of its natural substrates, phosphoenolpyruvate (PEP) and arabinose-5-phsophate (A5P), and with a mechanism-based inhibitor ($K_i = 0.4$ μM), directly characterizing the active site basic residues involved in the binding of their carboxylate and phosphate moieties. KDO8PS was labeled uniformly with ^{15}N or [η-$^{15}N_2$]Arg, and the ligands were selectively labeled with ^{13}C and ^{15}N. The NMR data established that PEP is bound by KDO8PS via a preserved set of structurally rigid and chemically unique Arg and Lys residues, with 5 Å (upper limit) between ϵ-^{15}N of this Lys and ^{31}P of PEP. A5P is bound in its cyclic forms to KDO8PS via a different set of Lys and Arg residues. The two sets arise from adjacent subsites that are capable of independent and sufficiently strong binding. The inhibitor is best characterized as an A5P-based substrate analogue inhibitor of KDO8PS. Five mutants in which highly conserved arginines were replaced with alanines were prepared and kinetically characterized. Our solid-state NMR observations complement the crystallographic structure of KDO8PS, and in combination with the mutagenesis results enable tentative assignment of the NMR-identified active site residues. Lys-138 and Arg-168 located at the most recessed part of the active site cavity are the chemically distinct and structurally rigid residues that bind PEP phosphate; R168A resulted in 0.1% of wild-type activity. Arg-63, exposed at the opening of the active site barrel, is the flexible residue with a generic chemical shift that binds A5P; R63A resulted in complete deactivation. The mechanistic implications of our results are discussed.

The enzyme 3-deoxy-D-*manno*-2-octulosonate-8-phosphate (KDO8P)[1] synthase (KDO8PS) (EC 4.1.2.16) catalyzes the condensation reaction between D-arabinose 5-phosphate (A5P) and phosphoenolpyruvate (PEP) to form KDO8P and inorganic phosphate (*1*) (Scheme 1). This important enzymatic reaction controls the carbon flow in the biosynthetic formation of an unusual eight-carbon sugar 3-deoxy-D-*manno*-2-octulosonate (KDO). KDO is an essential constituent of the lipopolysaccharide of all Gram-negative bacteria (*2*) and plays a crucial role in their assembly process (*2*, *3*). Since KDO is a site-specific constituent found only in Gram-negative organisms and is required for lipid A maturation and cellular growth, the inhibition of its production sets an attractive target for the design of novel antibacterial drugs.

Scheme 1

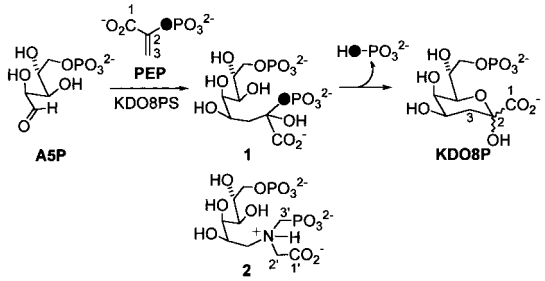

The mechanism of action of KDO8P synthase has been studied extensively. Although previous (*4*) and more recent (*5*, *6*) studies have established that the catalytic reaction of KDO8PS proceeds with the unusual cleavage of the C−O bond of PEP, its elementary steps were not identified. The cloning and overexpression of the *Escherichia coli* gene encoding KDO8PS have greatly facilitated mechanistic studies (*7*, *8*). By using stereospecifically 3-deuterio- and 3-fluoro-labeled analogues of PEP as alternative substrates of KDO8P synthase, it has been shown that the condensation step is stereospecific, involving the attachment of the si face of PEP to the re face of the carbonyl of A5P (*5*, *9*). Previous studies have demonstrated that the enzyme can act upon the

† This research was supported in part by the Israel Science Foundation, which was founded by the Israel Academy of Sciences and Humanities (A.S.), by the Foundation for Promotion of Research at the Technion (A.S. and T.B.), by U.S.-Israel Binational Science Foundation Grant 97-356 (T.B.), and by the Lady Davis Fellowship Trust (S.K.).

* To whom correspondence should be addressed: Department of Chemistry, Technion-Israel Institute of Technology, Haifa 32000, Israel. Fax: (972) 4 823-3735. E-mail for A.S.: chrschm@tx.technion.ac.il. E-mail for T.B.: chtimor@tx.technion.ac.il.

‡ Department of Chemistry and Institute of Catalysis Science and Technology.

§ Department of Food Engineering and Biotechnology.

[1] Abbreviations: KDO, 3-deoxy-D-*manno*-2-octulosonate; KDO8P, 3-deoxy-D-*manno*-2-octulosonate-8-phosphate; KDO8PS, KDO8P synthase; PEP, phosphoenolpyruvate; A5P, arabinose 5-phosphate; DAH7PS, 3-deoxy-D-*arabino*-2-heptulosonate-7-phosphate synthase; REDOR, rotational-echo double-resonance; CPMAS, cross polarization magic angle spinning.

10.1021/bi0017172 CCC: $19.00
Published on Web 11/10/2000

acyclic form of A5P and that the catalyzed reaction of KDO8P synthesis proceeds in a sequential manner with binding of PEP preceding that of A5P, and the release of P_i precedes that of KDO8P (*10*). More recently, it was shown that this reaction could also proceed via a random mechanism, in which A5P may bind first (*11*).

The application of pre-steady-state kinetic measurements using rapid-quench techniques, (*12*) in combination with chemical studies (*13*), supported a mechanism involving the formation of an acyclic reaction intermediate **1** (Scheme 1). In addition, we have recently synthesized the first bisubstrate inhibitor of the enzyme (*14*) that combines the key features of A5P and PEP into a single molecule and has an acyclic structure (structure **2**, Scheme 1). This compound proved to be the most potent inhibitor of KDO8PS with a K_d of 0.4 μM, whose substantial inhibition was interpreted as additional support for the concept of a mechanism that proceeds through the involvement of intermediate **1** (Scheme 1). Despite all the observations described above, there is no evidence available for the existence of **1** as a true intermediate. In a recent communication (*15*), we have reported the first direct identification of active site residues of KDO8PS by solid-state, rotational-echo double-resonance (REDOR) NMR (*16*). In parallel, the X-ray crystal structure of KDO8PS was determined in the presence of sulfate ions replacing the natural substrates (*17, 18*). This study identified the enzyme active site on the basis of its structural similarity to that of the previously determined X-ray structure of *E. coli* 3-deoxy-D-*arabino*-2-heptulosonate-7-phosphate synthase (*19*). On the basis of the active site architecture of KDO8PS as implied by the crystallographic study, it was suggested that the catalytic reaction proceeds via acyclic intermediate **1**, with A5P maintained in an open stretched form before it reacts with PEP.

Here, in continuation of our preliminary report (*15*), we present a detailed account of a REDOR solid-state NMR investigation of the active site of KDO8PS. In particular, the lyophilized binary complexes of KDO8PS with each of its natural substrates, and with bisubstrate inhibitor **2**, were studied. Identification of the active site residues involved in the binding of each substrate and of the inhibitor and their unique chemical and structural characteristics will be presented. The resulting mechanistic implications of the NMR data, combined with those resulting from the crystallographic study, will be drawn and discussed. Our approach employed preparation of [U-^{15}N]KDO8PS and [η-$^{15}N_2$]Arg-KDO8PS which were then subjected, alone and as binary complexes with [1-^{13}C]PEP, [1-^{13}C]A5P, [1′-^{13}C]**2**, and [3′-^{13}C,^{15}N]**2**, to a multinuclear (^{15}N, ^{13}C, and ^{31}P) solid-state NMR investigation. In particular, REDOR NMR as the principal means proved to be a powerful tool for the identification of the different residues involved in ligand binding, for their characterization, and for probing the state of the enzyme-bound ligands.

MATERIALS AND METHODS

General Methods. A5P was prepared enzymatically according to the procedure of Whitesides (*20*). The potassium salt of PEP was prepared in large quantities as previously described (*20*). [1-^{13}C]A5P was prepared from [1-^{13}C]-D-arabinose [96% ^{13}C, Cambridge Isotope Laboratories (CIL)] and hexokinase (Sigma). [1-^{13}C]PEP (99% ^{13}C) was purchased from CIL. $(^{15}NH_4)_2SO_4$ and [η-$^{15}N_2$]arginine were from Martek. 2-(Phosphonomethyl)acrylic acid (**3**) was purchased from Fluka. All other chemicals used in this study were purchased from Aldrich or from Sigma and were used without further purification. The specifically labeled glyphosate (Glp), [1-^{13}C]Glp (99% ^{13}C) and [3-^{13}C,^{15}N]Glp (99% ^{13}C and 99% ^{15}N), were the generous gift of J. Schaefer (Washington University, St. Louis, MO). Unlabeled **2** and its labeled variants were prepared by using a recently developed one-step procedure (*14*). This procedure employs the direct reductive amination in aqueous media between D-mannose 6-phosphate and glyphosate to provide **2** in one step. Using D-mannose 6-phosphate and the appropriately labeled glyphosates, we prepared [1′-^{13}C]**2** and [3′-^{13}C,^{15}N]-**2** in isolated yields [after ion-exchange chromatography on AG 1X8 (100−200 mesh, HCO_3^- form) eluted with a linear gradient (0 to 0.6 M) of triethylammonium bicarbonate buffer (pH 7.5), followed by passage through a column of Dowex 50W (K^+ form)] of 53 and 62%, respectively, as potassium salts.

Solution NMR Data. [1′-^{13}C]**2**: ^{1}H NMR (D_2O, pD 13.0, 400 MHz) δ 2.51 (d, 2H, J = 11.2 Hz, CH_2PO_3), 2.60 (dd, 1H, J = 13.3 and 7.85 Hz, H-1a), 2.82 (dd, 1H, J = 13.3 and 3.7 Hz, H-1b), 3.16 (dd, 1H, J = 16.4 and 4.1 Hz, NCHH$^{13}CO_2$), 3.26 (dd, 1H, J = 16.4 and 5.0 Hz, NCHH^{13}-CO_2), 3.61 (dd, 1H, J = 8.3 and 0.9 Hz, H-3), 3.63 (ddd, 1H, J = 8.0, 4.8, and 2.2 Hz, H-5), 3.68 (dd, 1H, J = 8.0 and 0.9 Hz, H-4), 3.69 (ddd, 1H, J = 8.3, 7.6, and 4.0 Hz, H-2), 3.76 (ddd, 1H, J = 11.5, 7.4, and 4.8 Hz, H-6a), 3.85 (ddd, 1H, J = 11.5, 6.5, and 2.2 Hz, H-6b); ^{13}C NMR (D_2O, pD 6.6, 100 MHz) δ 55.77 (d, J = 125.4 Hz, NCH_2P), 61.02 (d, J = 51.4 Hz, $NCH_2{}^{13}CO_2$), 61.81 (C1), 67.48, 68.61, 70.82, 72.37, 73.82, 173.11 ($^{13}CO_2$); ^{31}P NMR (proton-decoupled, D_2O, 81.0 MHz) pD = 6.6: δ 3.38 (CH_2OP), 6.89 (CH_2P); pD = 13.0: δ 5.44 (CH_2OP), 16.94 (CH_2P).

[3′-^{13}C,^{15}N]**2**: ^{1}H NMR (D_2O, pD 13.0, 400 MHz) δ 2.51 (dd, 2H, J = 127.4 and 11.0 Hz, $^{13}CH_2PO_3$), 2.60 (m, 1H, H-1a), 2.82 (bd, 1H, J = 14.7 Hz, H-1b), 3.15 (bd, 1H, J = 16.4 Hz, $^{15}NCHHCO_2$), 3.26 (bd, 1H, J = 16.4 Hz, $^{15}NCHHCO_2$), 3.58−3.84 (m, 6H, H-2, H-3, H-4, H-5, H-6a, H-6b); ^{13}C NMR (D_2O, 50.3 MHz) δ 55.42 (bd, J = 124.4 Hz, $^{15}N^{13}CH_2P$) (pD ∼7.0), 56.5 (bd, J = 143.1 Hz, $^{15}N^{13}$-CH_2P) (pD 13.0); ^{31}P NMR (proton-decoupled, D_2O, 81.0 MHz) pD ∼ 7.0: δ 5.46 (s, CH_2OP), 7.03 (bd, J = 126.7 Hz, $^{15}N^{13}CH_2P$); pD = 13.0: δ 5.45 (s, CH_2OP), 16.94 (dd, J_{C-P} = 143.1 Hz and J_{N-P} = 6.0 Hz, $^{15}N^{13}CH_2P$).

Overexpression and Purification of Enzymes. [U-^{15}N]-KDO8P synthase (specific catalytic activity of 9 units/mg) was isolated by overproduction of the *E. coli* DH5α (pJU1) strain, as previously described (*10*). The bacteria were grown on minimal medium containing 6 mg/mL KH_2PO_4, 12 mg/mL $Na_2HPO_4{\cdot}7H_2O$, 12.5 mg/mL $FeSO_4{\cdot}7H_2O$, 0.6 mg/mL glycerol, 0.25 mg/mL $MgSO_4$, 1 mg/mL thiamine, 1 mg/mL riboflavine, 1 mg/mL niacinamide, and 1 mg/mL pyridoxinmonohydrochloride, supplemented with 1.5 mg/mL [$^{15}N_2$]ammonium sulfate and 50 mg/mL ampicillin. The [η-$^{15}N_2$]Arg-KDO8PS in which all arginines are selectively labeled with [η-$^{15}N_2$]Arg was biosyntetically produced from an arginine auxotrophic strain W3679 (pJU1) grown in the same minimal medium mentioned above, and in addition was supplied with all amino acids at a concentration of 40 mg/

Table 1: Oligonuclotides Used for OC PCR Site-Directed Mutagenesis

mutation	sequence	site change
Arg-63 → Ala	5′-CAAAGCCAACGCGTCCTCCATCCACTC-3′	*Eco*RI to*Pst*I
Arg-70 → Ala	5′-CAC TCTTATGCGGGACCGGGCCTGG-3′	*Eco*RI to *Pst*I
Arg-168 → Ala	5′-GAAGTTAGCACCGGCGTCGCAAAGAATCAC-3′	*Pst*I to *Eco*RI
Arg-226 → Ala	5′-CTGAGCTAGCAGCAGCCGGTATGG-3′	*Eco*RI to *Pst*I
Arg-120 → Ala	5′-CGTTTCTTGCTGCGCAGACTGACCTGGTT-3′	*Eco*RI to *Pst*I

L, [η-$^{15}N_2$]Arg at a concentration 20 mg/L, and $(NH_4)_2SO_4$ at concentration of 4.9 g/L. The wild-type KDO8PS and all its labeled variants were purified according to the method previously reported by Ray (*1*) with slight modifications (*10*). All manipulations were carried out at 4 °C.

Enzyme Activity Assay. Unless otherwise stated, the enzyme activity was assayed in 1.0 mL of a reaction buffer consisting of 0.1 M Tris-HCl (pH 7.0), 0.2 mM PEP ($27K_m$), and 0.5 mM A5P ($20K_m$). Following equilibration at 37 °C for 2 min, KDO8PS (10 μL, at a final concentration of approximately 30 nM) was added, and the decrease in the absorbance difference between 232 and 350 nm (as the internal reference) was monitored as a function of time (MS-DOS UV/VIS software). This method (*21*) is based on the absorbance difference at 232 nm between PEP ($\epsilon = 2840$ M^{-1} cm^{-1}) and the other substrates and products ($\epsilon < 60$ M^{-1} cm^{-1}) under the assay conditions. The initial rate was calculated from a linear least-squares fit to the first 30 s of the progress curve. The concentrations of PEP, A5P, and **2** were determined precisely by quantitative assaying of the P_i released by alkaline phosphatase (*22*). In each case, to ensure complete hydrolysis of the phosphate monoester, the aliquots of the incubation mixture with alkaline phosphatase were tested by ^{31}P NMR. One unit of the enzyme activity is defined as the amount that catalyzes the consumption of 1 μmol of PEP/min at 37 °C. The protein concentrations of enzyme fractions were determined using the Bio-Rad protein assay with bovine serum albumin as a standard.

Preparation of Binary Complexes. Purified KDO8PS was exchanged into a buffer by extensive dialysis, 16−24 h, with two to six buffer replacements, containing 120 mM Mops (pH 7.3) and 0.1 mM DTT, and then concentrated by ultrafiltration through a Centricon concentrator to 150 μM. The enzyme concentration was determined according to the subunit molecular mass of 30 kDa (i.e., 1 mM = 30.0 mg/mL). The concentrated apoenzyme was rapidly frozen in liquid nitrogen and lyophilized. To prepare the binary complexes, the concentrated enzyme was incubated for 10 min at 4 °C with 1 equiv of either PEP, A5P, 2-(phosphonomethyl)acrylic acid (**3**), or inhibitor **2**. The final solution prior to lyophilization contained 150 μM KDO8PS, 0.4% PEG (polyethylene glycol 8000), 8 mM sucrose, and 3.8 mM MOPS. The solution containing the binary complex was divided into 8−10 mL aliquots each in a 250 mL flask. The aliquots were rapidly frozen in liquid nitrogen and lyophilized. Samples were completely freeze-dried within 16 h.

Site-Directed Mutagenesis. Mutagenesis was carried out by the overextension (OC) PCR mutagenesis method (*23*). Two separate reaction primers were run using flanking universal primers, the KS and T7 promoter primers (Stratagene), and internal mutagenesis primers (Table 1). The mutagenic PCR products were cleaved with two *Eco*RI and *Pst*I and cloned in vectors pKS^+ II (Stratagene), linearized with *Eco*RI and *Pst*I. The replacements were verified first by digestion of the DNA with appropriate restriction enzymes and by DNA sequencing. The corresponding proteins were produced and purified as described previously, using the vector pKSII-kdsa (instead of pJU1). *E. coli* W3679 (CGSC = 1184) was obtained from the *E. coli* genetic stock center. Site-directed mutagenesis was performed on five highly conserved arginines, to yield R63A, R70A, R120A, R226A, and R168A. In particular, kinetic characterization of R63A resulted in complete inactivation of the enzyme, while R70A, R120A, R168A, and R226A retained only 1.2, 0.1, 0.7, and 34% of the wild-type activity, respectively.

Spectral Methods. Spectrophotometric measurements were taken on a Hewlett-Packard 8452A diode array spectrophotometer using 1 cm path length cells with a thermostated cell holder and a circulating water bath at the desired temperature. ^1H NMR spectra were recorded on a Bruker AM-200 or AM-400 spectrometer, and chemical shifts (in ppm) are reported relative to HOD (δ 4.63) with D_2O as the solvent. ^{13}C NMR spectra were recorded on a Bruker AM-200 (50.3 MHz) or AM-400 (100.6 MHz) spectrometer, and the chemical shifts are reported relative to external sodium 2,2-dimethyl-2-silapentane sulfonate (δ 0.0) in D_2O. ^{31}P NMR spectra were recorded on a Bruker AM-200 spectrometer at 81.0 MHz, and the chemical shifts are reported relative to external orthophosphoric acid (δ 0.0) in D_2O. All the coupling constants (J) are in hertz.

Solid-State NMR Spectroscopy. NMR spectroscopy was carried out on a Chemagnetics/Varian 300 MHz CMX-*infinity* solid-state NMR spectrometer equipped with three radio frequency channels and a triple-resonance probe using 5 mm thin wall Zirconia rotors. Samples were spun at 5000 ± 2 Hz and were maintained at 1 ± 0.1 °C as a precaution throughout the experiments. Cross polarization magic angle spinning (CPMAS) echo experiments were carried out with a 5 μs ^1H 90°, 10 μs 180° pulse widths, a ^1H decoupling level of 100 kHz, and a repetition time of 2 s; Hartmann−Hahn rf levels were matched at 50 kHz, with 0.7, 2, and 2 ms contact times for ^{15}N, ^{13}C, and ^{31}P, respectively. The chemical shifts of ^{15}N, ^{13}C, and ^{31}P are reported relative to solid $(^{15}NH_4)_2SO_4$, TMS, and 85% H_3PO_4, respectively, with an accuracy of ±0.5 ppm. REDOR data were acquired using a REDOR pulse sequence with refocusing π pulses on each rotor period (T_R) on the observe channel and dephasing π pulses in the middle of each rotor period on the nonobserved nuclei, followed by an additional two-rotor period with chemical shift echo pulse in the middle. The REDOR pulses on both channels followed the xy-8 phase cycling scheme (*24*) to minimize chemical shift offset errors. REDOR data acquired with dephasing pulses are denoted S, while data without dephasing pulses serve for a reference and are denoted S_0. Difference data obtained via the $S_0 - S$ subtraction are denoted ΔS and yield spectra which exhibit peaks of dipolar-coupled chemical species exclusively. Cross polarization excitation was employed in all REDOR experi-

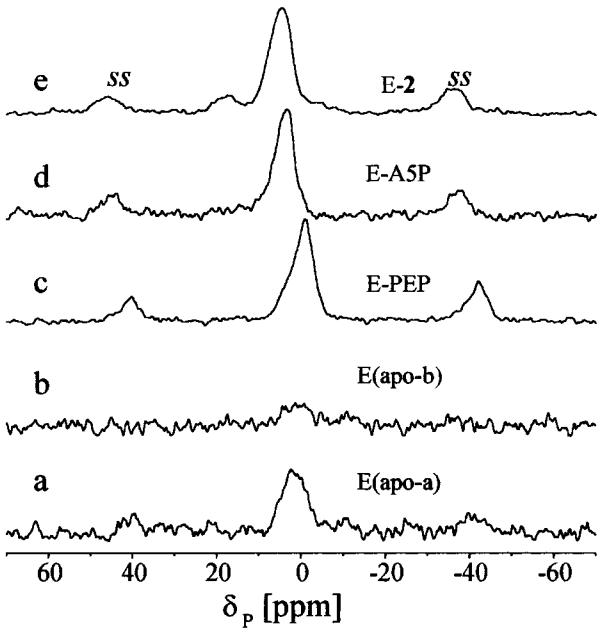

FIGURE 1: 121 MHz ^{31}P CPMAS NMR spectra of [U-^{15}N]KDO8P synthase alone following dialysis of 16 h (a) and 24 h (b) and of its binary complexes with PEP (c), A5P (d), and **2** (e). Spectra a and b are normalized with respect to spectrum c, accounting for enzyme weight. Apo-a and apo-b denote apoenzyme obtained after dialysis for 16 and 24 h, respectively. Spinning sidebands are denoted by *ss*.

ments using the parameters described above. Up to 80 000 scans were collected depending on sample weight and on the desired signal-to-noise ratio. Sample weights ranged between 70 and 200 mg, with the enzyme weight being about 40%.

RESULTS

Preparation of Apo-KDO8PS and Its Binary Complexes and Analysis by ^{31}P CPMAS NMR. Previous studies (*11*) have shown that KDO8P synthase is isolated with an equivalent of tightly associated PEP. To verify that all studied samples originate from an identical, PEP-free enzyme, the apoenzyme preparation procedure was monitored by both solution (not shown) and solid-state ^{31}P NMR. The ^{31}P CPMAS spectra of lyophilized KDO8PS following dialysis, the last step of the enzyme purification procedure prior to complex formation, are shown in parts a and b of Figure 1 after dialysis for 16 and 24 h with one and five dialysis buffer replacements, respectively. The spectra are normalized (accounting for enzyme weight in sample) with respect to the spectrum of the KDO8PS−PEP binary complex (Figure 1c) with a 1:1 stoichiometry. As can be seen, only the extensive dialysis is successful in removing most of the phosphate(s) present after enzyme purification. The ^{31}P peak in apoenzyme spectra 1a and 1b is centered at 2 ppm, which is about 3 ppm downfield from that of PEP in the binary complex (Figure 1c), and overlapping only its downfield tail. Its shifted position relative to that of PEP suggests that the majority of PEP is removed by the dialysis and that the observed residual phosphates are not PEP. While the exact chemical identity of these residual phosphates is not known to us yet, preliminary results (not shown) indicate that these do not bind tightly with basic enzyme residues or occupy the active site of KDO8PS.

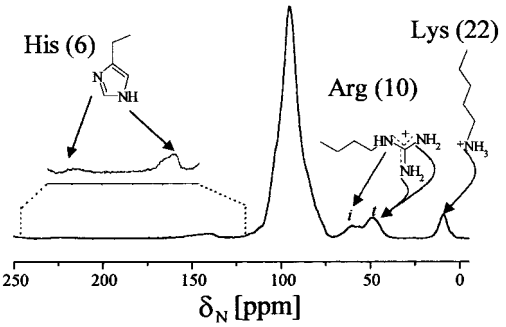

FIGURE 2: 30 MHz ^{15}N CPMAS NMR spectrum of the lyophilized binary complex of [U-^{15}N]KDO8P synthase with [1-^{13}C]PEP (for experimental conditions, see Materials and Methods). The abundance of each residue in KDO8PS is denoted in parentheses. The inset on the left is vertically expanded by a factor of 8.

Another approach to obtaining the apoenzyme, in which residual PEP is removed by adding excess A5P followed by dialysis, was attempted. However, employing ^{31}P solution NMR, we have found that A5P, when present as a binary complex with KDO8PS, could not be removed by a most extensive dialysis procedure (42 h, six dialysis buffer exchanges, 4 mL of enzyme solution in a total of 18 L of dialysis buffer). Its entire removal could be accomplished only via induction of its complete turnover by addition of excess PEP, therefore suggesting that the dissociation constant of the KDO8PS−A5P binary complex may be much lower than that of the KDO8PS−PEP complex.

In light of the findings presented above, the first method, which utilizes enzyme dialysis following the purification of the enzyme, was employed. As a practical compromise between enzyme loss upon extended dialysis periods and purity level, an intermediate stage between the two states reflected by spectra 1a and 1b was our routine procedure for the preparation of apoenzyme. Comprehensive discussion of the spectral details exhibited by each of the three binary complexes will be given below.

^{15}N CPMAS NMR of KDO8PS Binary Complexes. Uniformly ^{15}N-labeled enzymes give rise to typical ^{15}N NMR spectra in which the peaks of the side chains of the basic amino acids (Arg, Lys, and His) are resolved from the main peptide backbone peaks (*25*, *26*). [U-^{15}N]KDO8PS was obtained and used extensively throughout this work along with [η-$^{15}N_2$]Arg-KDO8PS and nonlabeled KDO8PS. The CPMAS ^{15}N NMR Hahn-echo spectrum of the [U-^{15}N]-KDO8PS binary complex with PEP (lyophilized powder) exhibits resolved peaks (Figure 2) for the nitrogen atoms of side chain histidine (nonprotonated, δ_1, 224 ppm; protonated, ϵ_2, 143 ppm), guanidino arginine (internal ϵ, 60 ppm; external η, 49 ppm), and side chain lysine (ϵ, 9 ppm). The intense peak at 95 ppm arises from 284 main chain peptide, 10 asparagine, and 13 glutamine side chain amide nitrogen atoms. In preparation for studying the active site of KDO8PS by REDOR NMR, the apoenzyme and the three binary complexes with PEP, A5P, and with **2** were prepared, and their ^{15}N CPMAS NMR spectra were compared as shown in Figure 3a−d (expanded chemical shift scale). Detailed inspection of the resolved arginine and lysine side chain peaks reveals fine structure for the arginine nitrogen at 56 ppm and a high-field shoulder at 3 ppm for the ϵ-nitrogen lysine, which are present in the spectra of all three complexes and of the apoenzyme (dotted lines). The relative integrated

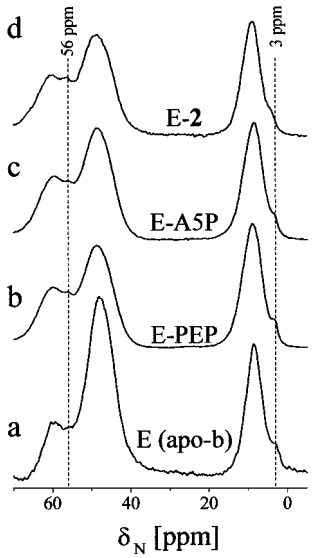

FIGURE 3: ^{15}N CPMAS NMR spectra, the arginine to lysine chemical shift region only, of lyophilized [U-^{15}N]KDO8PS alone (a) and of its lyophilized binary complexes (1:1 stoichiometric ratio) with [1-^{13}C]PEP (b), [1-^{13}C]A5P (c), and [1′-^{13}C]**2** (d). Apo-b denotes apoenzyme obtained after dialysis of 24 h. Dotted lines across the spectra correspond to arginine and lysine side chains residing in distinct chemical environments.

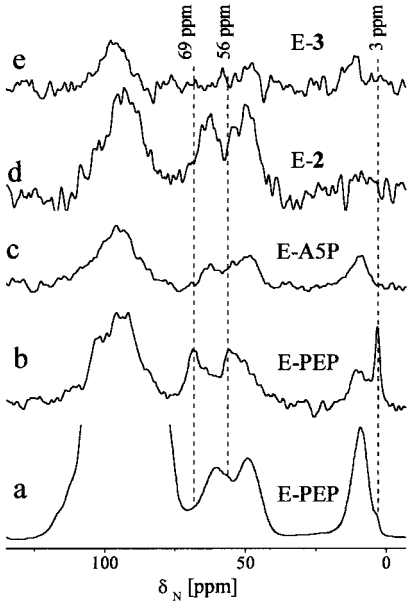

FIGURE 4: Reference, S_0 (a), and difference, ΔS (b), $64T_R$ ^{15}N-{^{31}P} REDOR NMR spectra of the [U-^{15}N]KDO8PS−[1-^{13}C]PEP binary complex. $64T_R$ ^{15}N{^{31}P} REDOR difference spectra of the [U-^{15}N]KDO8PS−[1-^{13}C]A5P (c), [U-^{15}N]KDO8PS−[1′-^{13}C]**2** (d), and [U-^{15}N]KDO8PS−**3** (e) binary complexes. The 69 ppm dotted line denotes a third distinct chemical environment exhibited by an internal guanidinium arginine nitrogen in spectrum b. Spectrum b is vertically expanded by a factor of 25 relative to its reference spectrum (a). Spectra c and d are expanded by the same factor relative to their respective reference spectra. **3** denotes the compound 2-(phosphonomethyl)acrylic acid.

intensity of the lysine upfield shoulder at 3 ppm corresponds to about 1/22 of the overall lysine peak, and is therefore attributed to a single unique lysine residing in a distinct chemical environment. The 56 ppm arginine peak is less resolved and therefore is harder to quantify, yet qualitatively, it can also be attributed to a single unique residue. Its unambiguous assignment to a substantially downfield-shifted terminal guanidino nitrogen was facilitated by NMR measurements applied to selectively labeled [η-^{15}N$_2$]Arg-KDO8PS complexes, where only the terminal arginine nitrogen atoms are labeled (vide infra).

Since the presence of these two unique peaks (56 and 3 ppm) of arginine and lysine residues is evident in the spectra of the three binary complexes (enzyme−PEP, −A5P, and −**2**) and in that of the apoenzyme as well (Figure 3), it therefore implies that they represent chemical environments of specific arginine and lysine residues which are not formed as a result of ligand binding, but rather pre-exist as unique microenvironments in the resting conformation of the substrate-free enzyme. These unique sites must result from the enzyme's primary through tertiary structure and, as will be shown below, are associated with specific recognition and binding of PEP by the enzyme.

Since at neutral pH both substrates and inhibitor **2** bear negatively charged groups, phosphate, carboxylate, and phosphonate, their charges must be counterbalanced by the positively charged basic residues at the enzyme's active site. Therefore, labeling the carboxylates of the ligands with ^{13}C, along with the naturally occurring ^{31}P in the phosphate and phosphonate moieties, set forth the basis for the identification of the basic residues which participate in their binding via REDOR NMR experiments. The REDOR technique (*16*) is based on the selective reintroduction of the dipolar interactions between pairs of specific types of nuclei, e.g., ^{15}N and ^{13}C. In this way, their selective identification is enabled, and in favorable cases, the accurate measurement of their dipolar interactions can also be performed, from which distance constraints can be obtained (*25*−*28*). Moreover, the ^{15}N spectral resolution offered for each of the basic residues allows us to screen them all simultaneously by employing uniform ^{15}N labeling of KDO8PS (*26*, *29*) rather than separate measurements of samples with residue-specific labeling.

REDOR experiments monitoring the ^{15}N enzyme nuclei as a function of their dipolar interactions, i.e., proximity, with neighboring ligand ^{31}P and ^{13}C nuclei serve as the primary source of information throughout the following work. These are complemented by ^{31}P and ^{13}C NMR experiments that directly monitor the state of the ligands themselves and their proximity to enzyme ^{15}N nuclei. These NMR results are described in detail below for each binary complex separately.

KDO8PS−*PEP Binary Complex.* Identification of the basic residues that participate in PEP phosphate binding is achieved via ^{15}N{^{31}P} REDOR experiments. Parts a and b of Figure 4 show the $64T_R$ REDOR spectra (only backbone to lysine side chain chemical shift region) of the [U-^{15}N]-KDO8PS−[1-^{13}C]PEP binary complex. The reference spectrum, S_0, shown in the lower trace is obtained following an echo time interval of $64T_R$ (with a T_R of 200 μs), without ^{31}P dephasing pulses. The spectrum in Figure 4b is the REDOR NMR difference spectrum ($\Delta S = S_0 - S$) which is vertically magnified by a factor of 25 relative to its reference spectrum (Figure 4a). This difference spectrum exhibits peaks exclusively for residues in the enzyme active site whose ^{15}N nuclei are within 6 Å of ^{31}P nuclei of the phosphate group. In addition to the broad difference peak of the amide nitrogens (95 ppm), Figure 4b exposes two lysine peaks at 3 and 9 ppm and two complex arginine peaks at 56 and 69 ppm. Thus, apart from the 56 ppm arginine and the 3 ppm

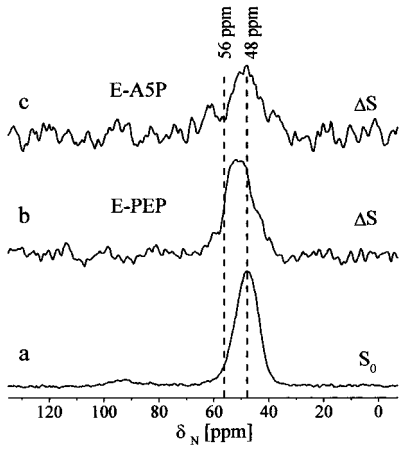

FIGURE 5: Reference (a) and difference (b) $64T_R$ $^{15}N\{^{31}P\}$ REDOR NMR spectra of the [η-$^{15}N_2$]Arg-KDO8PS−[1-^{13}C]PEP binary complex. (c) Difference $64T_R$ $^{15}N\{^{31}P\}$ REDOR NMR spectrum of the [η-$^{15}N_2$]Arg-KDO8PS−[1-^{13}C]A5P binary complex. The 56 ppm dotted line denotes the same chemical shift position as shown in Figures 3 and 4. The 48 ppm dotted line denotes the generic chemical shift position of the η-$^{15}N_2$ arginine moiety. Both difference spectra were vertically expanded by a factor of 10 relative to their normalized reference spectra.

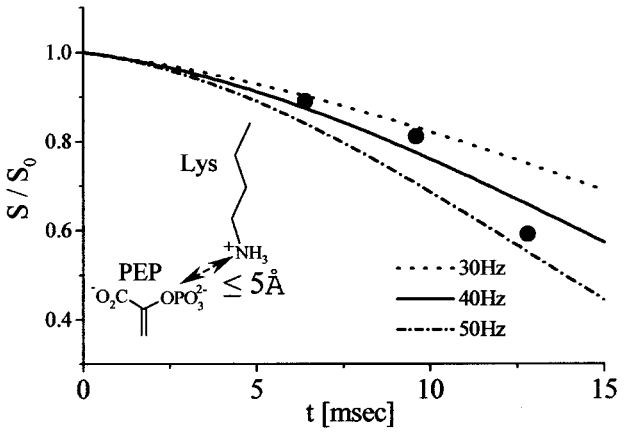

FIGURE 6: $^{15}N\{^{31}P\}$ REDOR dephasing, $S/S_0(n)$, for $n = 32$, 48, and 64 rotor cycles for the 3 ppm lysine difference peak of the [U-^{15}N]KDO8PS−[1-^{13}C]PEP complex (●). The three lines represent calculated dephasing curves for dipolar coupling strengths of 30, 40, and 50 Hz.

lysine peaks associated with chemically distinct enzyme environments as identified in Figure 3, this spectrum reveals a yet additional distinct environment manifested by the substantially downfield-shifted 69 ppm arginine peak (dotted lines). The spectrum in Figure 4b therefore identifies at least two different lysine residues, and at least two arginine guanidinium moieties that interact with PEP phosphate, where the role of the chemically distinct residues clearly stands out.

To sort out unambiguously whether the chemically shifted arginine peaks originate in a terminal or internal guanidino nitrogen, the [η-$^{15}N_2$]Arg-KDO8PS−[1-^{13}C]PEP binary complex was prepared and a $64T_R$ $^{15}N\{^{31}P\}$ REDOR NMR experiment was performed. Its reference and difference spectra shown in parts a and b of Figure 5 clearly manifest the asymmetric terminal arginine nitrogen peak (centered at 48 ppm) with its downfield sharp edge at 56 ppm, while the 69 ppm peak is absent. This difference spectrum (Figure 5b) therefore indicates that both peaks in Figure 4b, 56 and 69 ppm, are downfield shifted relative to their respective generic arginine chemical shifts, and that they correspond to terminal and internal guanidino arginine nitrogens, respectively. Geometrical considerations and the fact that these two difference peaks experience substantial downfield shifts strongly suggest that they originate in a single arginine residue (*30*).

It should be emphasized that the 3 ppm lysine difference peak (Figure 4b) is the narrowest one that is observed (30 Hz). The second lysine difference peak and those observed for the other two binary complexes (Figure 4c,d), for both arginine and lysine, give rise to difference peaks at least twice as broad (∼180 Hz). These larger line widths are attributed to larger conformational multiplicities or site heterogeneities experienced by the respective residues. Moreover, for the KDO8PS−PEP complex (Figure 4b), the arginine difference peaks are asymmetric, exhibiting sharper downfield edges, and must therefore represent complex peaks that arise from more than one residue. The steeper downfield edges reflect narrow internal and external guanidino peaks which arise from a single chemically distinct arginine residue (as is deduced for the upfield lysine peak), while the upfield, broad, and generic chemical shift part of their peaks arises from additional arginine residue(s). This group of narrow peaks (3, 56, and 69 ppm) reflects a lysine and an arginine which are conserved in the binding site in a unique and rigid conformation. This observation is also consistent with the observations of Radaev et al. (*17*, *18*), which suggest that PEP phosphate is bound at the most recessed part of the active site cavity, a region with limited conformational degrees of freedom.

Since the narrow difference peak at 3 ppm is unambiguously attributed to a single lysine residue, it enables a quantitative REDOR NMR determination of the $^{15}N-^{31}P$ internuclear distance in this binary complex. $^{15}N\{^{31}P\}$ REDOR NMR spectra were recorded as a function of the number of rotor cycles ($n = 32$, 48, and 64), from which the integrated intensity of the reference peak (S_0) for each n was estimated by deconvolution. The values of S/S_0 were then calculated as a function of n and are plotted in Figure 6 (●). Also shown are calculated REDOR dephasing curves for $^{15}N-^{31}P$ dipolar coupling strengths of 30, 40, and 50 Hz, corresponding to internuclear distances of 5.5, 5.0, and 4.6 Å, respectively. The experimental data are best fit by the 5.0 Å (40 Hz) calculated curve, assigning this distance to the internuclear separation between ^{31}P of PEP and the 3 ppm ϵ-lysine nitrogen atom. The scatter of the points within these limits suggests that the accuracy of this distance determination is ±0.4 Å. This distance determination relies on the assumption of full active site occupancy by PEP. Under the experimental conditions of complex preparation and if it is assumed that $K_d^{PEP} \cong K_m^{PEP} = 6\ \mu$M, one should anticipate 80−85% site occupancy. Therefore, our determined distance of 5.0 Å sets an upper limit for the internuclear separation (calculation of this REDOR-determined distance under the assumption of 80% active site occupancy yields a distance of 4.6 Å).

As an additional means of assessing whether the desired 1:1 stoichiometry is indeed maintained, we have estimated the ratio of the [1-^{13}C]PEP peak area (which is 100% ^{13}C-labeled) to the overall enzyme carbonyl peak (1.1% ^{13}C of 284 peptide bonds and 13 Gln, 10 Asn, 19 Glu, and 15 Asp

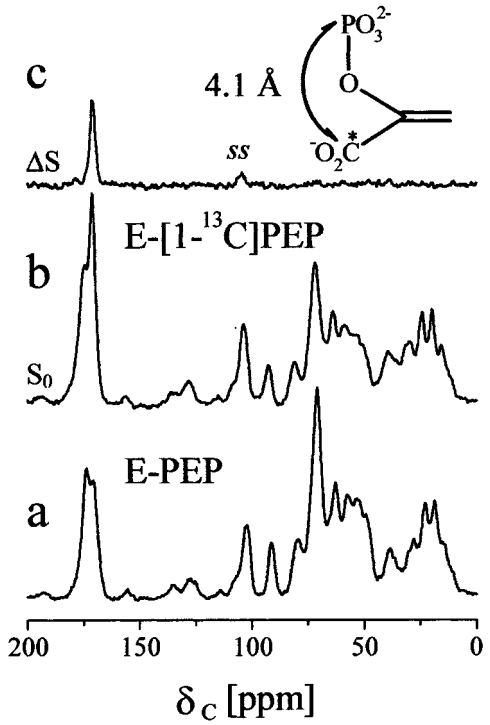

FIGURE 7: (a) 75 MHz ^{13}C CPMAS NMR spectrum of the binary complex of [U-^{15}N]KDO8P synthase with nonlabeled PEP. Reference (b) and difference (c) $32T_R$ $^{13}C\{^{31}P\}$ REDOR NMR spectra of the [U-^{15}N]KDO8PS−[1-^{13}C]PEP binary complex. Spinning sidebands are denoted by *ss*.

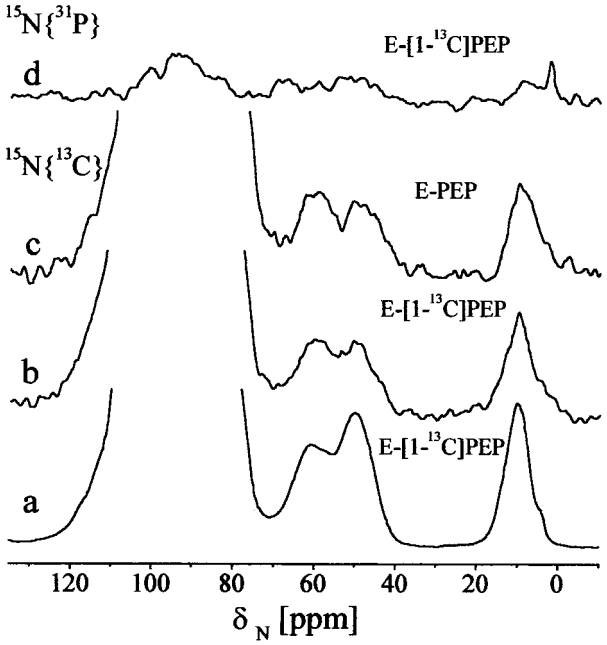

FIGURE 8: Reference (a) and difference (b) $32T_R$ $^{15}N\{^{13}C\}$ REDOR NMR spectra of the [U-^{15}N]KDO8PS−[1-^{13}C]PEP binary complex. (c) The $32T_R$ $^{15}N\{^{13}C\}$ REDOR difference spectrum of the binary complex with nonlabeled PEP ([U-^{15}N]KDO8PS−PEP). (d) The $32T_R$ $^{15}N\{^{31}P\}$ REDOR difference spectrum of the binary complex as in spectrum a. The difference spectra are vertically expanded by a factor of 20 relative to their reference spectra.

amide side chains). The theoretical value for a 1:1 mole ratio of PEP to KDO8PS in the binary complex is $(1 + 341 \times 0.011)^{-1} = 0.21$. The determination of the relative peak areas was carried out by recording the ^{13}C CPMAS NMR spectra of the complex with nonlabeled PEP (Figure 7a) and of the $32T_R$ $^{13}C\{^{31}P\}$ REDOR NMR spectra of the complex with [1-^{13}C]PEP [parts b (S_0) and c (ΔS) of Figure 7]. The REDOR difference spectrum (Figure 7c) identifies the 1-^{13}C carbonyl of PEP at 172 ppm, and allows its deconvolution from the ^{13}C CPMAS spectrum of the [U-^{15}N]KDO8PS−[1-^{13}C]PEP complex, from which a peak ratio of 0.19 was estimated, in good agreement with the theoretical value of 0.21. However, while this measurement confirms the overall stoichiometry, it should be noted that it cannot yield the fraction of bound versus unbound forms of the ligand.

To estimate the conformation of enzyme-bound PEP, we have conducted an additional $^{13}C\{^{31}P\}$ REDOR experiment with $48T_R$. From these two experiments (at $32T_R$ and $48T_R$), the C1−P dipolar coupling strength was estimated to be 178 Hz, from which an intramolecular C1−P distance of 4.1 Å is calculated. This distance matches the calculated (InsightII, MSI) maximum possible C1−P separation of 4.0 Å. The REDOR data therefore imply that in the binding site, the carboxylate and phosphate groups of PEP assume an exo conformation, i.e., C1, C2, O, and P of PEP lie in one plain (Figure 7, inset).

Generation of a complementary view, regarding which residues facilitate binding of the carboxyl group of PEP, was attempted via $^{15}N\{^{13}C\}$ REDOR experiments, now employing the 1-^{13}C label in PEP as the dephasing nuclei. Its $32T_R$ REDOR reference and difference spectra are depicted in parts a and b of Figure 8, respectively. The difference peaks present in this REDOR spectrum can be interpreted only when contributions arising from natural abundance ^{13}C nuclei, background dephasing, are accounted for (*28*, *31*). This is done by repeating the same $32T_R$ $^{15}N\{^{13}C\}$ REDOR experiment on a [U-^{15}N]KDO8PS−PEP binary complex, i.e., in the absence of the carboxylate 1-^{13}C label (Figure 8c). Within the given signal-to-noise ratio and resolution of the two difference spectra (Figure 8b,c), their comparison did not yield any quantifiable differences, and therefore does not allow us to identify particular enzyme residues that may interact with the carboxylate group of PEP. For comparison, the size and resolution of a difference peak due to a 40 Hz coupling are demonstrated for the 3 ppm lysine in the $32T_R$ $^{15}N\{^{31}P\}$ REDOR difference spectrum in Figure 8d. The absence of such a resolved difference peak in the $^{15}N\{^{31}C\}$ REDOR difference spectrum in Figure 8b does not allow us to determine if this 3 ppm lysine interacts with the carboxylate group of PEP (in addition to its interaction with PEP phosphate). Nevertheless, if it interacts with C1 of PEP, the dipolar coupling between the ^{13}C carboxylate and the 3 ppm ϵ-lysine nitrogen must be smaller than 40 Hz; i.e., their internuclear distance should be longer than 4.3 Å (if 80% active site occupancy is assumed, this limit becomes 3.8 Å). REDOR experiments with longer dephasing periods ($48T_R$ and $64T_R$) were performed as well, yet their limited sensitivity and resolution could not yield further information regarding the involvement of additional basic residues in carboxylate binding.

KDO8PS−A5P Binary Complex. Previous steady-state kinetic studies suggested an ordered mechanism with PEP binding first, followed by A5P (*10*). However, substrate trapping experiments have shown (*11*) that either PEP or A5P can bind to KDO8PS in a kinetically competent mode, suggesting a random mechanism. The implications of this

difference cannot be understood at this stage and require further study. To date, the dissociation constant of the KDO8PS−A5P binary complex is not known ($K_m^{A5P} = 26$ μM) (*10*), yet the difficulty encountered in removing A5P via dialysis (as described previously) suggests that A5P must be tightly bound to KDO8PS in the binary complex, with a dissociation constant lower than that of the enzyme−PEP complex. We will address the above issues in this section, focusing first on the identification of an enzyme's basic residues that interact with A5P phosphate via REDOR experiments with the [U-^{15}N]KDO8PS−[1-^{13}C]A5P binary complex.

The ^{15}N CPMAS and 64T_R ^{15}N{^{31}P} REDOR difference spectra of this binary complex are shown in Figures 3c and 4c, respectively. The latter exhibits peaks only for ^{15}N enzyme residues within 6 Å of the ^{31}P phosphate of A5P. In particular, the peaks of ϵ-lysine nitrogen (9 ppm), and two arginines (terminal and internal guanidino nitrogens at 49 and 62 ppm, respectively), are seen in addition to the broad amide backbone (95 ppm). The chemical shifts of these difference peaks are identical to those of the major (generic) peaks observed in the CPMAS NMR spectrum (Figure 3c). Clearly, these stand in marked contrast to the substantially shifted peaks observed in the REDOR NMR spectrum of the complex with PEP (Figure 4b), and therefore, they must correspond to a different set of specific residues. Moreover, in this spectrum, the three difference peaks are broader than those observed for the PEP complex, suggesting higher conformational heterogeneity of the interacting residues and/or involvement of several different (nonresolved) arginine residues. At the given experimental resolution, we are unable at this stage to determine whether each difference peak originates from a single residue or possibly from more, and therefore, quantitative distance constraints for A5P phosphate are not accessible. The 64T_R ^{15}N{^{31}P} REDOR NMR experiment performed on the [η-$^{15}N_2$]Arg-KDO8PS−[1-^{13}C]A5P complex isolates the terminal arginine difference peak as shown in Figure 5c, reproducing the data shown in Figure 4c.

It should also be noted that the relative difference peak strengths, $\Delta S/S_0$, of the lysine are about half the size of that of the terminal arginine. A5P phosphate binding is therefore facilitated mainly by the arginine residues via both terminal and internal guanidino nitrogens, and by weaker and/or fewer interactions with lysine residues. Both the domination of A5P binding by arginine versus lysine residues even though they are twice less abundant in KDO8PS (10 Arg vs 22 Lys residues) and the difficulty encountered in removing A5P by dialysis support the notion that we are probing specific binding of A5P within the enzyme's active site.

To further substantiate this conclusion, we have studied the [U-^{15}N]KDO8PS−**3** binary complex. Compound **3** is an isosteric phosphonate analogue of PEP which exhibits no inhibition, nor is it a substrate of KDO8PS (*32*). Therefore, it provides an example for a "nonligand" that would not form specific interactions with enzyme residues when prepared as a "binary complex". The 64T_R ^{15}N{^{31}P} REDOR NMR difference spectrum of this lyophilized 1:1 "complex" shown in Figure 4e exhibits a peptide backbone peak (95 ppm), a peak at the lysine position (9 ppm), and possibly a residual arginine peak (terminal, 48 ppm). The overall appearance of the smaller difference peaks in this spectrum and the fact that their relative intensities follow more closely the abundance of the basic residues in KDO8PS as reflected in their respective reference spectrum (not shown) suggest that they reflect a nonspecific binding. This observation further supports the attribution of the difference peaks in Figure 4b−d to specific interactions.

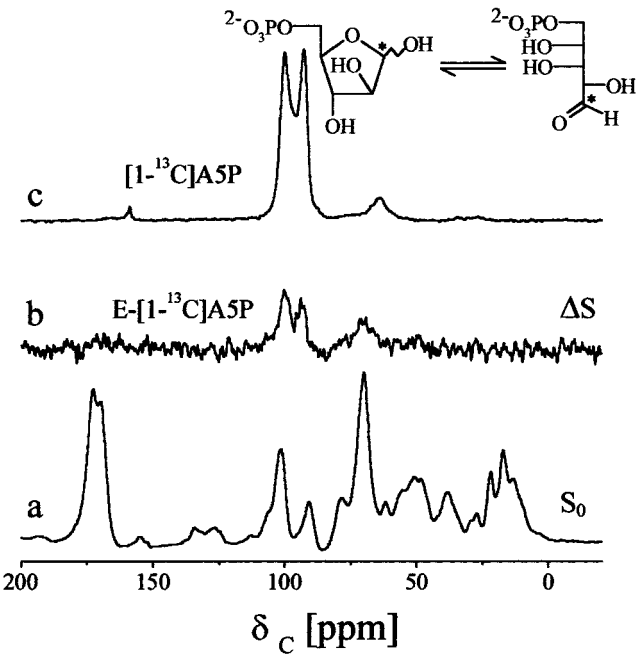

FIGURE 9: Reference (a) and difference (b) 64T_R ^{13}C{^{31}P} REDOR NMR spectra of the [U-^{15}N]KDO8PS−[1-^{13}C]A5P binary complex. (c) ^{13}C CPMAS NMR spectrum of lyophilized [1-^{13}C]A5P. The difference spectrum is vertically expanded by a factor of 10.

Previous studies (*10*), using 4-deoxy-A5P as an alternative substrate, have clearly demonstrated that KDO8PS can act directly on the acyclic aldehyde form of its substrate A5P. In aqueous solution at neutral pH, the aldehyde form of A5P is present at <0.2%, while the cyclic α and β anomers constitute 97.7% (57.3% α and 40.4% β) (*33*). Therefore, knowing whether the free aldehyde form of A5P is the only form that can bind to the enzyme, or the enzyme can also recognize and bind the cyclic forms of A5P, is important for the understanding of the catalytic mechanism. For this purpose, a 64T_R ^{13}C{^{31}P} REDOR NMR experiment was applied to the [U-^{15}N]KDO8PS−[1-^{13}C]A5P complex, utilizing the intramolecular ^{13}C−^{31}P dipolar interaction in [1-^{13}C]-A5P, thereby exposing only the peaks of the labeled C1 as shown in Figure 9 (a, S_0; b, ΔS). For comparison, the ^{13}C CPMAS spectrum of lyophilized [1-^{13}C]A5P is shown in Figure 9c, showing two major peaks of the α and β cyclic forms at 100 and 93 ppm, respectively, in close agreement with our ^{13}C solution data (103.5 and 97.7 ppm). The origin of the broad and less intense peak centered around 65 ppm (Figure 9c) and of the minor peak at 159 ppm (163.2 ppm in solution) could not be determined at this stage. The two major difference peaks shown in Figure 9b at 100 and 93 ppm are attributed to the α and β cyclic forms, respectively. Therefore, the pronounced peaks corresponding to the cyclic α and β anomeric forms, along with the absence of an aldehyde carbon reference and difference peak around 190−210 ppm (*34*) from spectra 9a and 9b, suggest that the major forms of enzyme-bound A5P are the cyclic forms. If the linear form is also present, it is too small to be detected and therefore could not exceed 20%.

KDO8PS−2 Binary Complex. The acyclic bisubstrate inhibitor **2** ($K_i = 0.4\ \mu M$) was designed to mimic the putative acyclic intermediate **1** by combining the key features of A5P and PEP into a single molecule, with the glyphosate moiety assuming the role of PEP. REDOR NMR experiments were employed to explore its actual mode of binding which leads to its high potency as an inhibitor.

The ^{15}N CPMAS spectrum of the binary complex of the [U-^{15}N]KDO8PS−[1′-^{13}C]**2** complex is shown in Figure 3d. The basic residues involved in binding the negatively charged phosphate and phosphonate moieties of **2** are sought via a $64T_R$ $^{15}N\{^{31}P\}$ REDOR experiment. In addition to the backbone nitrogen peak (95 ppm), its difference spectrum (Figure 4d) exhibits only arginine guanidino nitrogen peaks (terminal, 50 ppm; internal, 63 ppm) similar to those observed for the A5P complex in Figure 4c. Unlike PEP and A5P binding, no involvement of lysine residues in inhibitor binding is detected. This suggests that binding of **2** by the enzyme partially mimics A5P binding, and it has a little, if any, interaction at the PEP binding site. Furthermore, the presence of difference peaks of solely arginine residues for this binary complex emphasizes the fact that we are probing specific interactions.

To delineate the inhibitor's binding via its two different ^{31}P-bearing moieties, phosphate and phosphonate, ^{31}P CPMAS and REDOR NMR experiments were performed. The ^{31}P CPMAS spectrum of the [U-^{15}N]KDO8PS−[1′-^{13}C]-**2** binary complex shown in Figure 1e depicts two relatively broad peaks, 680 Hz wide, with an intense one centered at 5 ppm and a small one at 18 ppm, with an integrated intensity ratio of ca. 8:1. It should be noted that free **2** in neutral solution gives rise to 5.0 and 6.6 ppm peaks for phosphate and phosphonate (*14*), respectively, while that of the lyophilized inhibitor alone gives rise to a spectrum (not shown) similar to that obtained from the binary complex with the inhibitor (Figure 1e). Identification of the two ^{31}P peaks observed in spectrum 1e is accomplished by applying a $16T_R$ $^{31}P\{^{13}C\}$ REDOR NMR experiment to the KDO8PS−[3′-^{13}C,^{15}N]**2** binary complex as shown in parts a and b of Figure 10. Here, the strong intramolecular $^{31}P-3'-^{13}C$ dipolar interaction (a 1.86 Å P−C bond gives rise to a 1930 Hz dipolar coupling) yielded a difference spectrum (Figure 10b) showing exclusively two phosphonate peaks centered at 5 and 17 ppm, evidence of the presence of two phosphonate species. In attempts to further establish whether these species are involved in interactions with the enzyme (within 6 Å of the ^{15}N of enzyme residues or enzyme backbone), a $64T_R$ $^{31}P\{^{15}N\}$ REDOR NMR experiment was applied to the [U-^{15}N]KDO8PS−[1′-^{13}C]**2** binary complex. Its difference spectrum depicted in Figure 10c shows only one peak at 3.5 ppm, slightly shifted upfield with respect to the high-field (5 ppm) phosphonate in Figure 10b. This difference peak is attributed to the phosphate of **2**, it being the only ^{31}P moiety which is tightly bound by the enzyme. This observation substantiates the conclusion drawn from the $^{15}N\{^{31}P\}$ REDOR data depicted in Figure 4d, confirming that the phosphonate group in **2** which was originally designed to mimic PEP phosphate is not involved in tight interactions with any enzyme residues. It should also be noted that no interaction of a specific basic residue with the carboxylate moiety of **2** was detected via $^{15}N\{^{13}C\}$ REDOR experiments applied to the [U-^{15}N]KDO8PS−[1′-^{13}C]**2** and KDO8PS−[1′-^{13}C]**2** binary complexes (data not shown). Further evidence regarding the state of **2** in the KDO8PS−**2** binary complex is provided as Supporting Information.

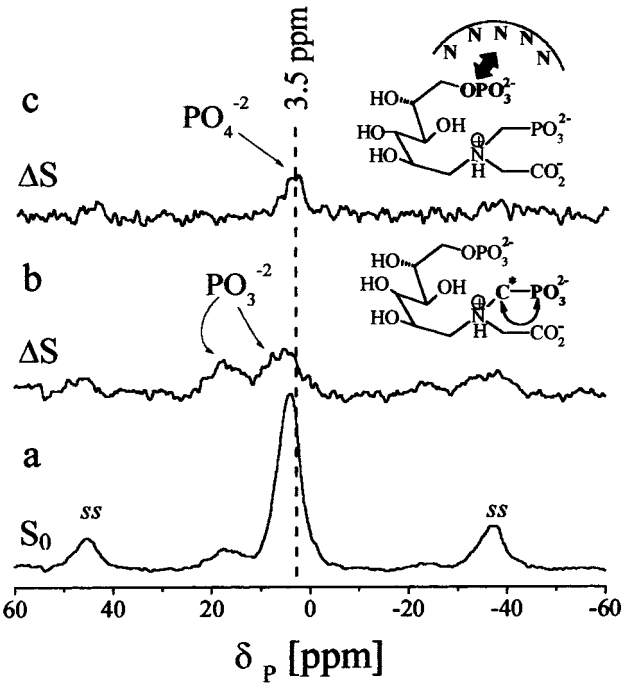

FIGURE 10: Reference (a) and difference (b) $16T_R$ $^{31}P\{^{13}C\}$ REDOR NMR spectra of the KDO8PS−[3′-^{13}C,^{15}N]**2** binary complex. (c) The $16T_R$ $^{31}P\{^{15}N\}$ REDOR difference spectrum of the [U-^{15}N]-KDO8PS−[1′-^{13}C]**2** binary complex. The dotted line denotes the chemical shift position of the difference peak in spectrum c. Spinning sidebands are denoted by *ss*.

^{31}P CPMAS NMR of the Binary Complexes. As in previous sections, ^{31}P CPMAS spectra were employed to monitor the state of the inhibitor in the KDO8PS−**2** complex and the residual phosphates with the apoenzyme and the ^{31}P CPMAS NMR spectra of the two binary complexes with the natural substrates were recorded and are shown in parts c and d of Figure 1. The spectra of [U-^{15}N]KDO8PS−[1-^{13}C]PEP and [U-^{15}N]KDO8PS−[1-^{13}C]A5P complexes depict relatively broad peaks, ∼650 Hz wide, centered at −1 and 3.3 ppm, respectively. Free PEP in neutral solution gives rise to a −0.2 ppm peak while that of free A5P to a 4.3 ppm peak.

It is of note that all three binary complexes (Figure 1c−e) exhibit excessive ^{31}P peak breadths of about 650 Hz. This extensive width is in marked contrast to observations made by Schaefer and co-workers (*35*) in their study of lyophilized EPSPS−S3P−Glp ternary complexes. Narrow ^{31}P spectral lines (≤120 Hz) served as criteria for the minimal conformational heterogeneity of the substrates within the active site, and were shown to depend strongly on the lyophilization conditions. In our study so far, efforts to optimize lyophilization parameters did not result in reduced line widths. However, in all the samples prepared via this procedure, the enzyme maintained 70−80% of its specific activity even after being subjected to solid-state NMR measurements and storage for 4−6 months at −20 °C.

Contributions to the peak could also arise in part from partial population of ligands which do not occupy the active site, or from residual phosphates as were observed in the apoenzyme spectra (Figures 1a,b), yet these could not be the only source for the ^{31}P peak width. Therefore, the ^{31}P

CPMAS spectra imply that there is a certain degree of heterogeneity of the ligands within the active site. Thus, both the ^{31}P CPMAS spectra and ^{15}N REDOR difference spectra imply that both the active site residues and the ligands possess a certain degree of heterogeneity. The distinct set of narrow ^{15}N peaks of the lysine and arginine residues that bind PEP is therefore the exception in this study, drawing further attention to their rigidly preserved chemical and structural environment. The reproducibility of our experimental results from different preparations and from altered procedures ensures that the detected heterogeneities are not degrading the interpretation of the data.

DISCUSSION

Our REDOR NMR investigation of the binary complexes of KDO8PS with each of its natural substrates, PEP and A5P, has identified two different sets of enzyme residues that bind the phosphate groups of each ligand. Each of these two sets is capable of sufficiently strong and independent binding. These observations are in accordance with previous studies (*11*) that showed that either PEP or A5P can bind first to KDO8PS to carry out chemical catalysis. The two observed sets of basic enzyme residues exhibit vastly different structural and chemical characteristics. Of the set of residues that interact with PEP phosphate, in particular, one lysine (3 ppm) and one arginine (56 and 69 ppm) reside in a rigid and chemically distinct environment. Interestingly, the unique chemical and structural state of these residues is preserved in the apoenzyme as well as in the other binary complexes, regardless of whether PEP, A5P, or inhibitor **2** is bound in the active site. Unlike the rigid PEP-binding environment, the set of arginine and lysine residues that interact with A5P phosphate exhibits larger conformational heterogeneity. This suggests that the residues that bind A5P phosphate are located on a more exposed enzyme surface where higher flexibility is possible. It should be noted that these structural characteristics reflect the state of the binding sites in solution: the rapid freezing of binary complexes and their subsequent lyophilization freeze these states and prevent any flexibility thereafter.

Via REDOR NMR, we determined that the arginine guanidino groups employ both the terminal and internal (η and ϵ) nitrogen atoms in their interactions with the negatively charged phosphates of both PEP, A5P, and **2**. This binding mode of the arginine side chain is well-known from crystallographic studies of biological systems (*36*) and was also encountered and identified in solid-state NMR studies (*29*, *30*).

After our initial report on the solid-state NMR study of KDO8PS (*15*), the crystal structure of KDO8PS (*17*) with sulfate ions occupying its active site, and so substituting for the phosphate groups of the natural substrates, was reported. Both studies, the crystallographic and the solid-state NMR, are in excellent agreement and constitute together a more comprehensive description of the organization of the active site of KDO8PS and its mechanistic details. The crystallographic study reports (*17*) that PEP phosphate binds at the most recessed part of the active site cavity by Lys-138 and Arg-168; A5P phosphate binding occurs in a raised position above the opening of the barrel by Arg-63 and Ser-64. Our observations regarding the rigidity of the residues that bind PEP in contrast to the flexibility of those which bind A5P may be well understood in view of their location in the active site; the buried residues that bind PEP are deprived of conformational degrees of freedom, while those above the opening are not spatially restricted. Maintaining for PEP a rigid and chemically distinct binding site reflects the more critical role of recognition and binding of PEP in a more hindered location within the enzyme.

Furthermore, the crystallographic data, along with our site-directed mutagenesis results, allow us to tentatively assign the NMR-identified active site residues. The chemically distinct lysine and arginine residues (denoted by the dotted lines in Figure 4b) that bind PEP are assigned as Lys-138 and Arg-168, which is supported by the almost complete inactivation of mutant R168A (0.1% of the *wt* activity). The arginine, which dominates A5P binding, is assigned as Arg-63, which is supported by the complete inactivation exhibited by mutant R63A.

The NMR results showed that one more lysine (9 ppm peak in Figure 4b) and one more arginine (composed peak), at least, are involved in binding PEP phosphate. Involvement of additional basic residues in A5P phosphate binding is not implicitly suggested or excluded (Figure 4c). On the basis of the tertameric crystal structure of KDO8PS (*17*), the most proximate contacts of basic residues with the sulfates that correspond to substrate phosphates are as follows. Arg-120 is 8.66 (η_1) and 6.15 Å (η_2) from PEP and A5P, respectively. This arginine reaches to the active site from an adjacent subunit, and its mutation, R120A, resulted in almost complete inactivation (0.7% of the *wt* activity); this combination of observations supports the notion that the active solution form of KDO8PS is a tetramer. Lys-60 and Lys-55 are found 7.2 and 7.9 Å, respectively, from PEP phosphate; Lys-154 is 8.0 Å from A5P phosphate and is reaching over from the adjacent subunit. These three are conserved lysine residues, of which Lys-60 and Lys-55 were suggested (*17*) to interact with the carboxylate group of PEP (yet could not be detected by the ^{13}C{^{31}P} REDOR NMR experiments due to their limited sensitivity). It is likely that within these most proximate residues (Arg-120, Lys-50, Lys-60, and Lys-154) which are highly conserved and/or essential, some contribute to the difference spectra in parts c and d of Figure 4, yet the definite assignment is not possible at this time. While determining whether these or others are the putative interacting residues cannot be done at this stage, the size of the lysine difference peak at 9 ppm (Figure 4b) calls for a proximity ($<$6 Å) much closer than that indicated by the X-ray data. We therefore suggest that the ultimate structure of the active site with the native substrates may be arranged slightly different from that reported with the sulfate ions (*17*), where other more intimate contacts with substrate phosphates should be present.

REDOR NMR data show that both the α- and β-furanose forms of A5P, which constitute over 97% of its anomers in solution, are also the primary forms which are bound to KDO8PS in the binary complex. Since it was already demonstrated (*10*) (using 4-deoxy-A5P as an alternative substrate) that the aldehyde form of A5P can both bind and react, the immediate consequence of the NMR data described above is that bound cyclic A5P should be able to convert to its acyclic reactive form for the reaction to occur. This conversion may be induced by PEP binding or, alternatively,

Scheme 2: Proposed Elementary Steps for the KDO8PS-Catalyzed Reaction

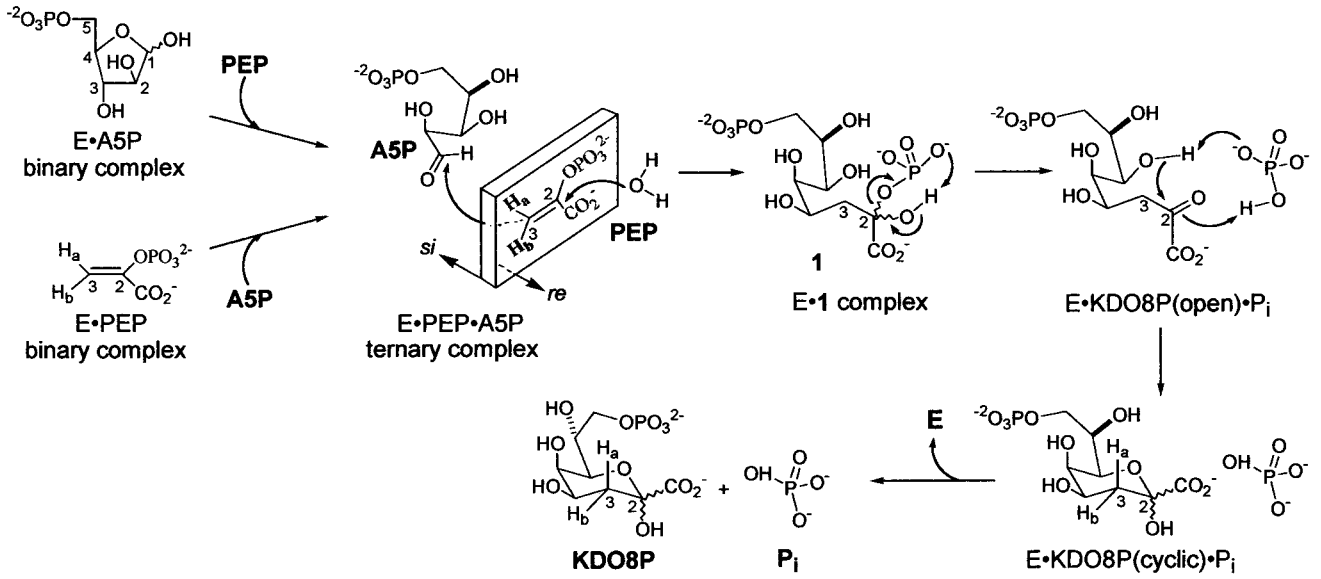

if A5P's dynamic mutarotation, cyclic ⇌ acyclic, continues uninterrupted while A5P is enzyme-bound. Indeed, it has been shown that the ring opening rate constants for free A5P in solution (*33*) are one order of magnitude higher than the k_{cat} of KDO8PS (*10*). Since KDO8PS is capable of binding both the α and β anomers of A5P, it is conceivable that no enzyme involvement should be required for their distinction, or for the activation of ring opening. Alleviation of this "cost-ineffective" requirement is made possible if the 1-hydroxyl of (α and β) A5P has a minor role in the recognition and binding of A5P's cyclic forms, leaving this side of A5P free to undergo ring opening. The actual ring-opening mechanism cannot be inferred from the current binary complex data.

Substrate trapping experiments conducted under single-enzyme turnover conditions have shown (*11*) that KDO8PS can carry out chemical catalysis via a random mechanism. Its implication is that either PEP or A5P can bind to KDO8PS in a kinetically competent mode and that one ligand is not interfering with the binding of the other. It is possible that A5P, by binding above the opening of the active site cavity in its cyclic forms, provides sufficient free space for PEP to access the cavity and bind. Then, when ring opening takes place, the proximity would be correct for catalysis to occur. Access of PEP might be limited if A5P would bind only in its linear form, with its aldehyde pointing down toward the cavity. Full clarification of this issue requires additional experimental evidence.

The REDOR NMR data for inhibitor **2** show that its binding to the enzyme is facilitated mainly by its phosphate in a way that partially mimics that of A5P binding, while its phosphonate moiety which was designed to mimic PEP does not form any intimate interactions with enzyme basic residues, or with the backbone. The enzyme employs only arginine residues to bind the phosphate of **2**, similar to A5P where arginines are forming the dominant part of the interactions. Hence, we conclude that the glyphosate part of **2** may block the cavity entrance and restrict PEP's free access to its own site, resulting in PEP-competitive inhibition (*14*). Therefore, **2** is neither a good bisubstrate mimic nor a good mimic of intermediate **1**, and it can be best characterized as an A5P-based substrate analogue inhibitor of KDO8PS.

On the basis of all the results described above, and in combination with the earlier results accumulated through the synthesis and evaluation of various analogues of A5P (*10*, *37*), PEP (*5*, *12*, *38*), and of the product KDO8P (*7*, *13*, *38*) as mechanistic probes, we propose for the synthase-catalyzed reaction the elementary steps illustrated in Scheme 2. While the pathways leading to the formation of the E−PEP−A5P ternary complex are consistent with the random mechanism, the timing and overall stereochemistry of the condensation step are still unresolved issues. Therefore, either a synchronous generation of new C−C and C−O bonds or a stepwise process can be suggested as a possible mechanism for the formation of acyclic intermediate **1**. In addition, although the stereochemistry of the C−C bond formation is well-documented (*si* face of PEP toward the *re* face of C1 of A5P), the C−O bond between C2 of PEP and a water oxygen can form either syn or anti to that of the newly formed C−C bond (only anti shown in Scheme 2). This leads to a new stereogenic center at C2 of acyclic intermediate **1** whose absolute configuration is not known.

In the phosphate elimination process (Scheme 2), we suggest that the base-catalyzed proton abstraction from the hydroxyl group is effected by a base provided by the substrate, namely, one of the phosphate peripheral oxygens. This proposed progression in **1** combines several advantages: (i) a strong base from the phosphate monoester is used for proton abstraction, (ii) an enzyme base need not be brought close to the charged phosphate and carboxylate groups, (iii) the expected steric hindrance associated with the removal of a proton from a tertiary hemiketal hydroxyl is avoided, and (iv) the direct transfer of the proton from the hydroxyl to the phosphate oxygen improves the effectiveness of the phosphate as a leaving group. Furthermore, this type of proton abstraction intramolecularly catalyzed by the phosphate (or phosphonate) oxygens has precedence in the reaction catalyzed by dehydroquinate synthase (*39*).

Last, the scenario we suggest for the early release of P_i followed by KDO8P release (*9*) follows the same line as described for the free access of PEP while A5P is bound in its cyclic form. Inorganic phosphate, after its cleavage from the E−I complex, may assist the ring closure upon formation

of the cyclic pyranose form of KDO8P, before it can escape through the top of the barrel. Its release may not be interrupted by cyclic KDO8P, which is bound via its phosphate moiety at the top of the active site cavity. Inhibition shown by a series of KDO8P analogues with cyclic pyranose structures that are prohibited from undergoing ring opening (*7*, *13*, *38*) further supports the proposed scenario.

The proposed mechanism in Scheme 2 can explain the unusually high rate of turnover of the enzyme with (*E*)-3-fluoro-PEP as the alternative substrate (*9*). In addition, it also offers an explanation for the catalysis of phosphate ester hydrolysis, and may even answer the long-standing question regarding the preferred cleavage of the C−O bond over the P−O bond of PEP, adopted by this enzyme. Thus, unlike the EPSPS (*40*, *41*) and UDP-GlcNAc enolpyruvoyl transferase reactions (*42*), in which a similar C−O bond cleavage of PEP and the formation of inherently stable intermediates have been well-documented, in the case of KDO8PS it seems that the enzyme forms a very unstable hemiketal phosphate (*43*, *44*) intermediate (**1**), and its subsequent decomposition may occur with no further involvement of the enzyme. Further studies are underway to assess the mechanistic pathway as proposed in Scheme 2. Also in progress is the synthesis of new analogues of putative intermediate **1**.

ACKNOWLEDGMENT

We thank Prof. J. Schaefer from the Department of Chemistry, Washington University, for the kind gift of [1-^{13}C]Glp and [3-^{13}C,^{15}N]Glp employed for the synthesis of labeled **2**. We thank Dr. N. Adir from the Department of Chemistry, Technion, for most insightful and helpful discussions.

SUPPORTING INFORMATION AVAILABLE

The state of **2** in the KDO8PS−**2** binary complex characterized by ^{13}C{^{31}P} REDOR spectra of the [U-^{15}N]-KDO8PS−[1′-^{13}C]**2** and KDO8PS−[3′-^{13}C,^{15}N]**2** binary complexes, along with ^{15}N{^{31}P} REDOR spectra of the KDO8PS−[3′-^{13}C,^{15}N]**2** binary complex. This material is available free of charge via the Internet at http://pubs.acs.org.

REFERENCES

1. Ray, P. H. (1980) *J. Bacteriol. 141*, 635−644.
2. Anderson, L., and Unger, F. M., Eds. (1983) *Bacterial Lipopolysaccharides*, ACS Symposium Series 231, American Chemical Society, Washington, DC.
3. Inouye, M. (1979) in *Bacterial Outer Membrane: Biogenesis and Function*, Wiley, New York.
4. Hedstrom, L., and Abeles, R. (1988) *Biochem. Biophys. Res. Commun. 157*, 816−820.
5. Dotson, G. D., Nanjappan, P., Reily, M. D., and Woodard, R. W. (1993) *Biochemistry 32*, 12392−12397.
6. Dotson, G. D., Dua, R., Clemens, J., Wooten, E. M. D., and Woodard, R. W. (1995) *J. Biol. Chem. 270*, 13698−13705.
7. Bassov, T., Sheffer-Dee-Noor, S., Kohen, A., Jakob, A., and Belakhov, V. (1993) *Eur. J. Biochem. 217*, 991−999.
8. Woisetschlager, M., and Hogenauer, G. (1986) *J. Bacteriol. 168*, 437−439.
9. Kohen, A., Berkovich, R., Belakhov, V., and Baasov, T. (1993) *Bioorg. Med. Chem. Lett. 3*, 1577−1582.
10. Kohen, A., Jakob, A., and Baasov, T. (1992) *Eur. J. Biochem. 208*, 443−449.
11. Liang, P., Lewis, J., Anderson, K. S., Kohen, A., D'Souza, W. F., Benenson, Y., and Baasov, T. (1998) *Biochemistry 37*, 16390−16399.
12. Benenson, Y., Belakhov, V., and Baasov, T. (1996) *Bioorg. Med. Chem. Lett. 6*, 2901−2906.
13. Sheffer-Dee-Noor, S., Belakhov, V., and Baasov, T. (1993) *Bioorg. Med. Chem. Lett. 3*, 1583−1588.
14. Du, S., Faiger, H., Belakhov, V., and Baasov, T. (1999) *Bioorg. Med. Chem. 7*, 2671−2682.
15. Kaustov, L., Kababya, S., Du, S., Baasov, T., Gropper, S., Shoham, Y., and Schmidt, A. (2000) *J. Am. Chem. Soc. 122*, 2649−2650.
16. Gullion, T., and Schaefer, J. (1989) *J. Adv. Magn. Reson. 13*, 57−83.
17. Radaev, S., Dastidar, P., Patel, M., Woodard, R. W., and Gatti, D. L. (2000) *J. Biol. Chem. 275*, 9476−9484.
18. Radaev, S., Dastidar, P., Patel, M., Woodard, R. W., and Gatti, D. L. (2000) *Acta Crystallogr. D56*, 516−519.
19. Shumilin, I. A., Kretsinger, R. H., and Bauerle, R. H. (1999) *Structure 7*, 865−875.
20. Hirschbein, B. L., Mazenod, F. P., and Whitesides, G. M. (1982) *J. Org. Chem. 47*, 3765−3766.
21. Schoner, R., and Herrmann, K. M. (1976) *J. Biol. Chem. 251*, 5440−5447.
22. Ames, B. N. (1966) *Methods Enzymol. 8*, 115−118.
23. Meza, N., Nunez-Valdez, M. E., Sanchez, J., and Bravo, H. (1996) *FEMS Microbiol. Lett. 145*, 333−339.
24. Gullion, T. G., Baker, D. B., and Conradi, M. S. (1990) *J. Magn. Reson. 89*, 479−484.
25. McDowell, L. M., Schmidt, A., Cohen, E. R., Studelska, D. R., and Schaefer, J. (1996) *J. Mol. Biol. 256*, 160−171.
26. Goetz, J. M., Poliks, B., Studelska, D. R., Fischer, M., Kugrlbrey, K., Bacher, A., Cushman, M., and Schaefer, J. (1999) *J. Am. Chem. Soc. 121*, 7500−7508.
27. Hing, A. W., Tjandra, N., Cottam, P. F., Schaefer, J., and Ho, C. (1994) *Biochemistry 33*, 8651−8661.
28. McDowell, L. M., Klug, C. A., Beusen, D. D., and Schaefer, J. (1996) *Biochemistry 35*, 5395−5403.
29. Li, Y., Appleyard, R. J., Shuttleworth, W. A., and Evans, J. N. S. (1994) *J. Am. Chem. Soc. 116*, 10799−10800.
30. Petkova, A. T., Hu, J. G., Bizounok, M., Simpson, M., Griffin, R. G., and Herzfeld, J. (1999) *Biochemistry 38*, 1562−1572.
31. Garbow, J. R., and Gullion, T. (1995) in *Carbon 13 NMR Spectroscopy of Biological Systems*, pp 65−115, Academic Press, New York.
32. Kohen, A. (1994) Ph.D. Thesis, Technion, Haifa, Israel.
33. Pierce, J., Serianni, A. S., and Barker, R. J. (1985) *J. Am. Chem. Soc. 107*, 2448−2456.
34. Seriani, A. S., Pierce, J., Huang, S. G., and Barker, R. (1982) *J. Am. Chem. Soc. 104*, 4037−4044.
35. Christensen, A. M., and Schaefer, J. (1993) *Biochemistry 32*, 2868−2873.
36. Salunke, D. M., and Vijayan, M. (1981) *Int. J. Pept. Protein Res. 18*, 348−351.
37. Ray, P. H., Kelsey, J. E., Bigham, E. C., Benedict, C. D., and Miller, T. A. (1983) *ACS Symp. Ser. 231*, 141−170.
38. Baasov, T., and Kohen, A. (1995) *J. Am. Chem. Soc. 117*, 6165−6174.
39. Bender, S. L., Widlanski, T., and Knowles, J. R. (1989) *Biochemistry 28*, 7560−7572.
40. Anderson, K. S., Sikorski, J. A., Benesi, A. J., and Johnson, K. A. (1988) *J. Am. Chem. Soc. 110*, 6577−6579.
41. Anderson, K. S., Sikorski, J. A., and Johnson, K. A. (1988) *Biochemistry 27*, 7395−7406.
42. Marquardt, J. L., Brown, E. D., Walsh, C. T., and Anderson, K. S. (1993) *J. Am. Chem. Soc. 115*, 10398−10399.
43. Haddad, J., Vakulenko, S., and Mobashery, S. (1999) *J. Am. Chem. Soc. 121*, 11922−11923.
44. Rendina, A. R., and Cleland, W. W. (1984) *Biochemistry 23*, 5157−5168.

BI0017172